ACCOUNTS of chemical research

Article

pubs.acs.org/accounts

Multinuclear Group 4 Catalysis: Olefin Polymerization Pathways Modified by Strong Metal−Metal Cooperative Effects

Jennifer P. McInnis, Massimiliano Delferro,* and Tobin J. Marks*

Department of Chemistry, Northwestern University, Evanston, Illinois 60208-3113, United States

CONSPECTUS: Polyolefins are produced today catalytically on a vast scale, and the manufactured polymers find use in everything from artificial limbs and food/medical packaging to automotive and electrical components and lubricants. Although polyolefin monomers are typically cheap (e.g., ethylene, propylene, α-olefins), the resulting polymer properties can be dramatically tuned by the particular polymerization catalyst employed, and reflect a rich interplay of macromolecular chemistry, materials science, and physics. For example, linear low-density polyethylene (LLDPE), produced by copolymerization of ethylene with linear α-olefin comonomers such as 1-butene, 1-hexene, or 1-octene, has small but significant levels of short alkyl branches (C_2, C_4, C_6) along the polyethylene backbone, and is an important technology material due to outstanding rheological and mechanical properties. In 2013, the total world polyolefin production was approximately 211 million metric tons, of which about 11% was LLDPE. Historically, polyolefins were produced using ill-defined but highly active heterogeneous catalysts composed of supported groups 4 or 6 species (usually halides) activated by aluminum alkyls. In 1963, Karl Ziegler and Giulio Natta received the Nobel Prize for these discoveries. Beginning in the late 1980s, a new generation of group 4 molecule-based homogeneous olefin polymerization catalysts emerged from discoveries by Walter Kaminsky, a team led by James Stevens at The Dow Chemical Company, this Laboratory at Northwestern University, and a host of talented groups in Germany, Italy, Japan, the United Kingdom, and the United States. These new "single-site" catalysts and their activating cocatalysts were far better defined and more rationally tunable in terms of structure, mechanism, thermodynamics, and catalyst activity and selectivity than ever before possible. An explosion of research advances led to new catalysts, cocatalysts, deeper mechanistic understanding of both the homogeneous and heterogeneous systems, macromolecules with dramatically altered properties, and large-scale industrial processes.

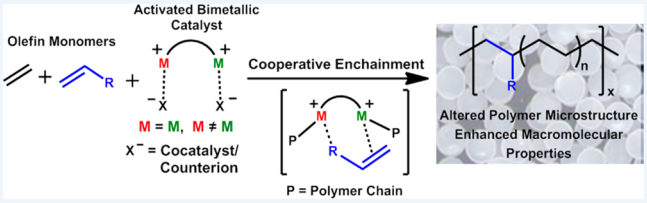

It is noteworthy that many metalloenzymes employ multiple active centers operating in close synergistic proximity to achieve high activity and selectivity. Such enzymes were the inspiration for the research discussed in this Account, focused on the properties of multimetallic olefin polymerization catalysts. Here we discuss how modifications in organic ligand architecture, metal···metal proximity, and cocatalyst can dramatically modify polyolefin molecular weight, branch structure, and selectively for olefinic comonomer enchainment. We first discuss bimetallic catalysts with identical group 4 metal centers and then heterobimetallic systems with either group 4 or groups 4 + 6 catalytic centers. We compare and contrast the polymerization properties of the bimetallic catalysts with their monometallic analogues, highlighting marked cooperative enchainment effects and unusual polymeric products possible via the proximate catalytic centers. Such multinuclear olefin polymerization catalysts exhibit the following distinctive features: (1) unprecedented levels of polyolefin branching; (2) enhanced enchainment selectivity for linear and encumbered α-olefin comonomers; (3) enhanced polyolefin tacticity and molecular weight; (4) unusual 1,2-insertion regiochemistry for styrenic monomers; (5) modified chain transfer kinetics, such as M-polymer β-hydride transfer to the metal or incoming monomer; (6) LLDPE synthesis with a single binuclear catalyst and ethylene.

1. INTRODUCTION

Proximate catalytic centers in many multimetallic enzyme active sites play an essential role in turnover frequency and substrate/product selectivity.[1−3] Likewise, solution-phase abiotic bimetallic catalysts have emerged as powerful mediators of asymmetric transformations,[4−6] epoxidations,[7] enantioselective cycloadditions,[8] and coordinative polymerizations.[9−12] Bimetallic olefin polymerization catalysts can exhibit marked metal···metal cooperative effects versus their monometallic analogues in how monomers are enchained to produce macromolecules, and while these effects are apparent in catalytic activity, polymer microstructure (molecular weight, chain branching, monomer repeat regioregularity), and selectivity for comonomer enchainment, the actual mechanistic details are just emerging. This Account describes recent research at Northwestern in which the effects of metal position in the Periodic Table, ligand architecture, ligand electronic characteristics, and metal−metal distance are investigated and analyzed with respect to the polymeric structures produced.

2. BIMETALLIC "CONSTRAINED GEOMETRY" POLYMERIZATION CATALYSTS

Mononuclear constrained geometry catalysts[13] (CGCs, Chart 1A) emerged in the 1990s as versatile ethylene polymerization catalysts

Received: April 24, 2014
Published: July 30, 2014

   dx.doi.org/10.1021/ar5001633 | Acc. Chem. Res. 2014, 47, 2545−2557

Chart 1. Examples of (A) Monometallic Constrained Geometry Catalysts and Mononuclear Cocatalysts and (B) Bimetallic Constrained Geometry Catalysts and Binuclear Cocatalysts

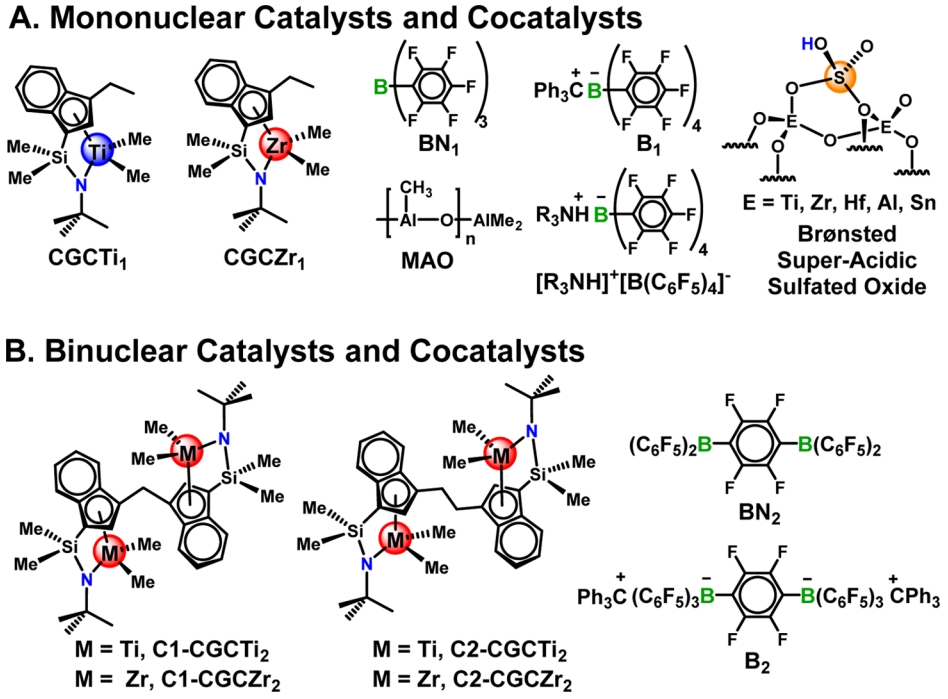

Scheme 1. Examples of Organo-Group 4 Catalyst Activation Processes with (A) Methylaluminoxanes, (B) Perfluoroarylborane, (C) Perfluoroarylborate, and (D) Sulfated Metal Oxide Cocatalyst/Activator

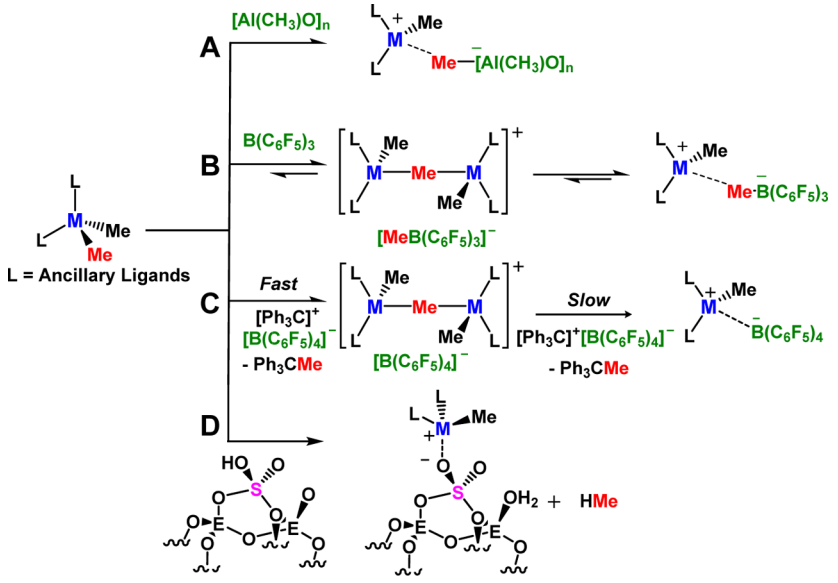

with high polymerization activities and the unusual propensity to enchain bulky comonomers, reflecting sterically open, coordinately unsaturated architectures, and to achieve high polymer molecular masses, reflecting relatively slow rates of process by which terminate chain growth (chain-transfer). Activation of these metal "precatalysts" with borane/alane, alkylaluminoxanes such as methylaluminoxane (MAO), solid superacidic supports,[14,15] or borate/aluminate cocatalysts (Chart 1A) is essential to create the active catalysts—highly electron-deficient ion pairs (Scheme 1).[16−18]

Group 4 metals are widely employed in mononuclear CGC catalysts, with polymerization activity approximately scaling as Ti > Zr > Hf. A representative binuclear CGC synthesis (Chart 1B) is shown in Scheme 2, with free ligand metalation achieved by $M(NMe_2)_4$ (M = Ti, Zr) protodeamination, and subsequent reaction with $AlMe_3$ or Me_3SiCl to afford the corresponding dimethyl or dichloro precatalysts, respectively. The crystal structures of C1-CGCZr$(NMe_2)_4$ and C2-CGCZr$(NMe_2)_4$ (Figure 1) reveal significant differences in Zr···Zr distances between the methylene- and ethylene-bridged complexes.[19] Furthermore, methylene-bridged C1-CGCZr$_2$ has a large computed indenyl-CH_2-indenyl rotational barrier (~65 kcal/mol), enforcing a proximal conformation of the Zr centers onto the same side of the molecule, and a minimum estimated Zr···Zr distance of ~7.06 Å.[20] In contrast, ethylene-bridged C2-CGCZr$_2$ has a

dx.doi.org/10.1021/ar5001633 | Acc. Chem. Res. 2014, 47, 2545−2557

Scheme 2. Synthetic Route to Binuclear Group 4 Constrained Geometry Precatalysts

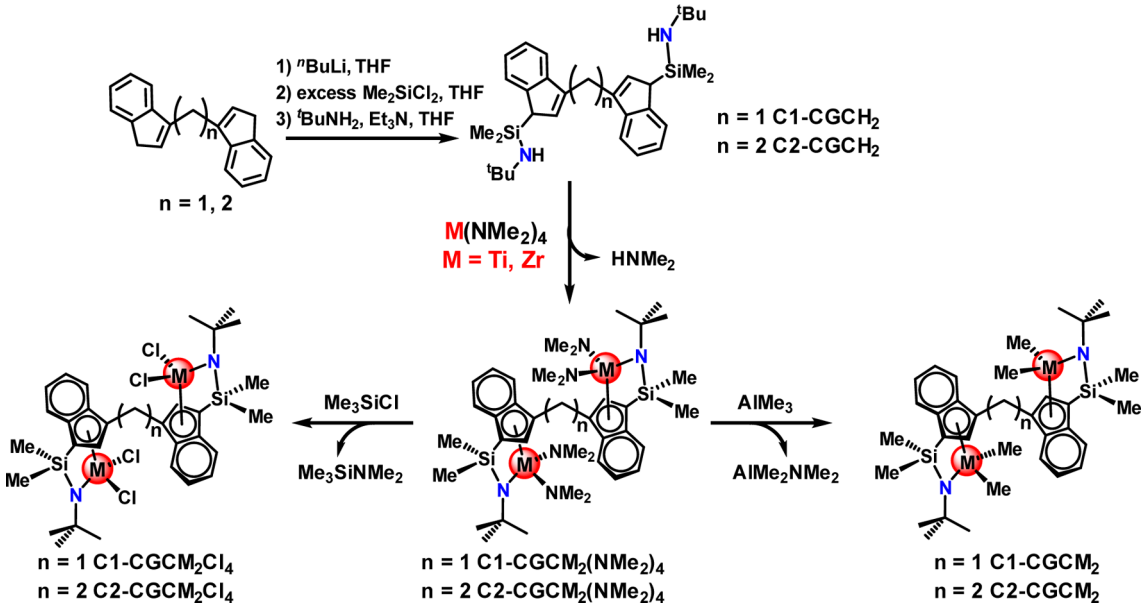

Table 1. Ethylene Homo- and Copolymerization Data Mediated by Catalysts $CGCZr_1$, C1-$CGCZr_2$, and C2-$CGCZr_2$[a]

entry	catalyst	cocatalyst	comonomer	activity[b]	M_n (kg/mol)[c]	ethyl branches (/1000C)[d]	*n*-butyl branches (/1000C)[d]
1	$CGCZr_1$	B_1	–	127	0.61[e]	1.1	0
2	$CGCZr_1$	B_2	–	93	0.63[e]	6.5	0.6
3	C2-$CGCZr_2$	B_1	–	87	0.76[e]	2.7	0
4	C2-$CGCZr_2$	B_2	–	63	1.1[e]	12	1.0
5	C1-$CGCZr_2$	B_1	–	19	21.5	1.3	0
6	C1-$CGCZr_2$	B_2	–	13	32.6	1.6	0
7	$CGCZr_1$	B_2	1-hexene	133	0.73[e]	6.0	3.2
8	C1-$CGCZr_2$	B_2	1-hexene	8.6	22.1	1.3	17.2
9	C2-$CGCZr_2$	B_2	1-hexene	87	1.1[e]	10	5.5
10	$CGCZr_1Cl_2$	MAO		25	0.95[e]	0	0
11	C1-$CGCZr_2Cl_4$	MAO		25	244	0	0
12	C2-$CGCZr_2Cl_4$	MAO		23	268	0	0
13	$CGCZr_1$[f]	B_2		680	2.4	1.7	1.1
14	C1-$CGCZr_2$[f]	B_2		640	2.4	2.8	1.4
15	C2-$CGCZr_2$[f]	B_2		560	3.1	7.0	2.4
16	$CGCZr_1$[f]	B_2	1-hexene	840	3.8	1.7	35.1
17	C1-$CGCZr_2$[f]	B_2	1-hexene	570	3.8	2.2	48.3
18	C2-$CGCZr_2$[f]	B_2	1-hexene	780	2.5	5.6	44.9

[a]Polymerizations in 100 mL of toluene with 10 μmol of monometallic catalyst and 5 μmol of bimetallic catalyst at constant 1.0 atm ethylene. [b]Units: kg PE mol $[Zr]^{-1}$ atm^{-1} h^{-1}. [c]GPC versus polystyrene standards. [d]^{13}C NMR spectral analysis. [e]^{1}H NMR spectral analysis. [f]C_6H_5Cl polymerization solvent.

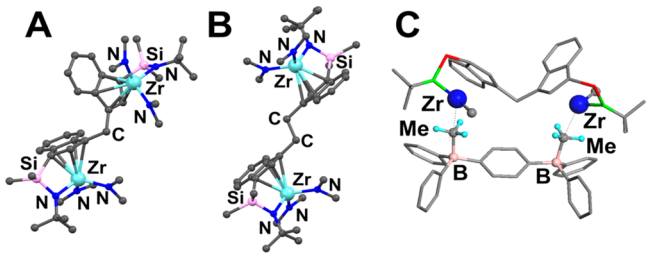

Figure 1. Molecular structures of (A) C1-$CGCZr(NMe_2)_4$. Adapted with permission from ref 19. Copyright 2005 American Chemical Society. (B) C2-$CGCZr(NMe_2)_4$. Adapted with permission from ref 24. Copyright 2002 American Chemical Society. (C) DFC1-$CGCZr_2$ activated with B_2; computed by DFT. Adapted with permission from ref 26. Copyright 2009 American Chemical Society.

negligible computed rotational barrier, a crystallographically derived Zr···Zr distance of 8.671(3) Å, and likely conformers with shorter distances. Activation of these complexes with strongly Lewis acidic perfluoroarylmetalloids, methylalumoxane (MAO), trityl salts, or strong Brønsted acids with weakly coordinating counteranions such as $[R_3NH]^+[B(C_6F_5)_4]^-$ generates highly electrophilic ion-paired catalysts. In addition, solid oxide supports such as sulfated alumina facilitate metal hydrocarbyl chemisorption on highly Brønsted acidic sites resulting in facile M–C σ-bond protonolysis.[21] Note that the ion-pairing is largely electrostatic, energetically non-negligible in low dielectric solvents and, for mononuclear catalysts, strongly modulates polymerization and chain termination/transfer rates as well as the stereochemistry of prochiral monomer enchainment.[22,23] In regard to binuclear catalysts, DFT results reveal close catalyst–cocatalyst ion pairing (e.g., Figure 1C), and greater ion-pair

dx.doi.org/10.1021/ar5001633 | Acc. Chem. Res. 2014, 47, 2545–2557

Scheme 3. Plausible Mechanistic Scenario for Cooperative Ethylene Polymerization at Bimetallic Constrained Geometry Catalytic Centers

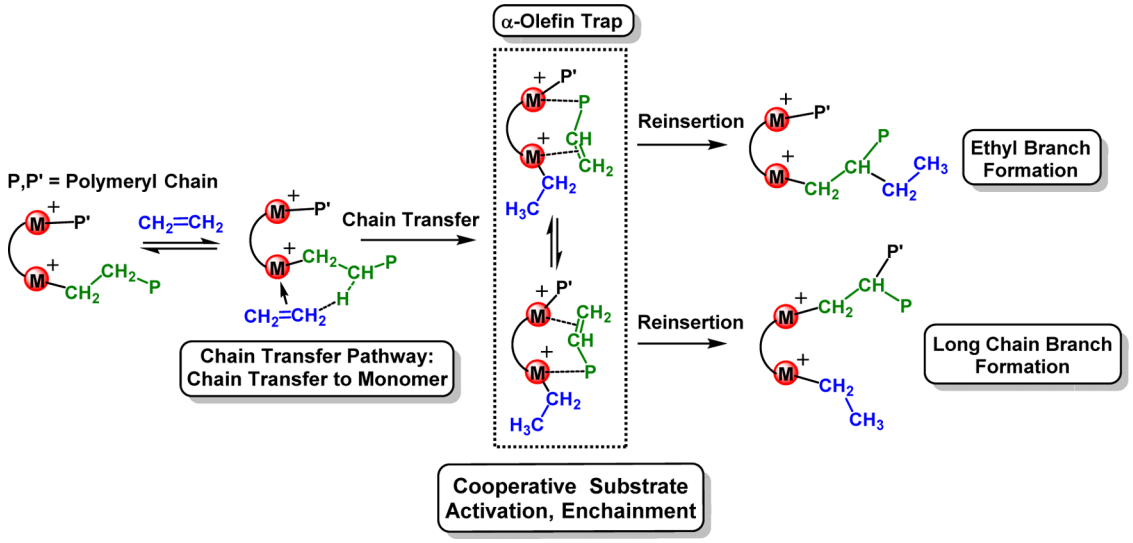

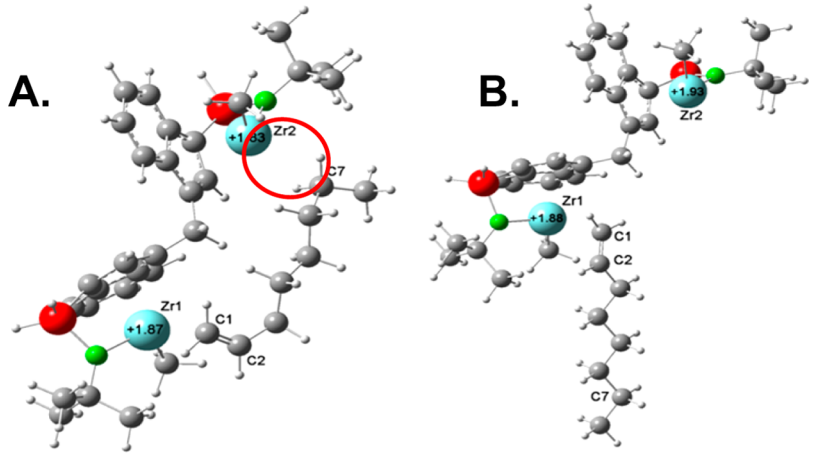

Figure 2. DFT-derived structure of C1-CGCZr$_2^{2+}$ + 1-octene: (A) with Zr1-olefin π-bonding + a (C7)-H···Zr2 agostic interaction indicated in red, and (B) with Zr1-olefin π-bonding only. Adapted with permission from ref 26. Copyright 2009 American Chemical Society.

dissociation energies versus the mononuclear analogues due to stronger dication-counterdianion electrostatic attraction.

Olefin polymerizations were conducted first with the aforementioned bimetallic Zr polymerization catalysts[24,25] using mononuclear and binuclear activators, and the results compared with the mononuclear analogues. Product polyethylene M_w's are found to be essentially independent of ethylene pressure, implicating chain growth termination by transfer of a Zr$^+$-CH$_2$CH$_2$R β-hydrogen to incoming ethylene, forming CH$_2$═CHR and a new Zr$^+$-CH$_2$CH$_3$ active center. Interestingly, while polymerization activity versus mononuclear CGCZr$_1$ is depressed, bimetallic C2-CGCZr$_2$ and C1-CGCZr$_2$ (activated by B$_2$) afford polyethylenes with 1.7× and 52× greater M_w's, respectively (Table 1, entries 2, 4, 6). This suggests that the C2-CGCZr$_2$/C1-CGCZr$_2$ increased M···M proximity suppresses the chain termination rate versus chain growth.

Moreover, the polyethylenes produced by the bimetallic catalysts have significantly greater branching, with a preponderance of ethyl branching, indicating favorable chain transfer to monomer, followed by α-olefin/polymer reinsertion (Scheme 3). The largest cooperative enchainment effects versus mononuclear controls are achieved with B$_2$-activated catalysts. When C2-CGCZr$_2$ is activated by B$_2$ as compared to B$_1$, the product polymer M_w increases by 1.4×, the total branch content is increased by 4.8×, while the catalytic activity decreases by 1.4× (Table 1, entries 3, 4). The increased M_w and branch content with the binuclear activator can be explained by a closer activated Zr···Zr distance and electrostatically optimized ion pair spatial conformations which hold the propagating chains in close proximity (Scheme 3).

In addition to the distinctive polyethylene microstructures produced by the bimetallic Zr catalysts, ethylene + 1-hexene copolymerizations further illuminate cooperative enchainment effects in the bimetallic CGC catalysts. Under identical reaction conditions, C2-CGCZr$_2$ enchains significantly greater amounts of 1-hexene than does CGCZr$_1$, evident in the higher *n*-butyl branching in the product polymer (Table 1, entries 7, 9). C1-CGCZr$_2$ incorporates the highest 1-hexene density, 17.2 *n*-butyl branches/1000C. A similar trend is observed with 1-pentene copolymerizations where, under the same conditions, C2-CGCZr$_2$ introduces 11 *n*-propyl branches/1000C while CGCZr$_1$ only introduces 3.3 propyl branches/1000C. These results support the argument that proximity-related Zr···Zr

dx.doi.org/10.1021/ar5001633 | Acc. Chem. Res. 2014, 47, 2545−2557

effects increase α-olefin comonomer enchainment selectivity via a bimetallic α-olefin trapping mechanism (Scheme 3).

Further insight into bimetallic enchainment effects is provided via DFT modeling of 1-octene interactions with activated C1-CGCZr$_2$.[26] These reveal that the olefin is bound by C=C coordination to one Zr center and an alkyl C−H···Zr agostic binding to the other cationic center (Figure 2A), computed to be ∼2 kcal/mol more stable than the non-agostic structure (Figure 2B). Furthermore, the C7—H bond in structure A is elongated by ∼0.02 Å, and the effective Zr$_2$ charge (+1.83) is substantially lower than that in B (+1.93), supporting the presence of agostic σ-donation. Note also that these agostic interactions are also operative when shorter α-olefins (e.g., 1-pentene, 1-hexene) are employed as the comonomer.[26] It is argued that such agostic interactions are at least partially responsible for the unusual enchainment properties of the bimetallic catalysts, and that multiple electrophilic metal centers can cooperatively bind/activate α-olefins. Specifically, the greater polyethylene product branch densities produced by the bimetallic catalysts are reasonably correlated with agostic-assisted intramolecular reinsertion processes (Scheme 3). Furthermore, the observed increased α-olefin comonomer enchainment effected by the bimetallic catalysts is in accord with this picture, and that the modified catalytic environment of two proximate centers increases relative propagation: termination rates, favoring increased product M_w's.

Significant differences in polymerization characteristics are also evident on changing the cocatalyst from a borate to methylaluminoxane (MAO).[17−19] With MAO, ethylene polymerization activity falls for monometallic CGCZrCl$_2$ and bimetallic C2-CGCZr$_2$Cl$_4$ catalysts by ∼3−5× while M_w increases substantially (Table 1, entries 10−12). On the other hand, the C1-CGCZr$_2$Cl$_4$ catalyst activity is not significantly affected by change in cocatalyst/activator. This behavior likely reflects steric and/or spatial arrangement effects around the binuclear catalyst C1-CGCZrCl$_4$. ^{13}C NMR polymer end-group analysis suggests that chain transfer to Al is not the major growth termination step here (i.e., M−Polymeryl + Al−Me = M−Me + Al−Polymeryl). Furthermore, ^{1}H NMR studies of C1-CGCZr$_2$ + MAO reveal a signal assignable to a Zr(μ-methyl)−Zr$^+$ moiety,[25] and suggests that the two Zr centers can in principle achieve close proximity during polymerization, stabilized by the bulky MAO cocatalyst/counteranions. This type of structure is plausibly connected with the enhanced M_w's. The influence of catalyst/cocatalyst ion pairing strength was also probed by varying the polymerization solvent from toluene (ε = 2.38) to more polar C$_6$H$_5$Cl (ε = 5.68), and realizing dramatically increased polymerization activities, despite similar ethylene solubility. In ethylene homopolymerizations, the activities enhancement is ∼50× for C1-CGCZr$_2$ + B$_2$, ∼9× for C2-CGCZr$_2$ + B$_2$, and ∼7× for CGCZr$_1$ + B$_2$ in C$_6$H$_5$Cl versus toluene (Table 1, entries 13−15). That the activities of all three catalysts are now comparable in C$_6$H$_5$Cl suggests that catalyst/cocatalyst ion paring is significantly weakened in the higher dielectric solvent, allowing less restricted olefin enchainment. In ethylene/1-hexene copolymerizations, the comonomer incorporation selectivity for both mononuclear and binuclear catalysts increases significantly in C$_6$H$_5$Cl versus toluene: ∼3× for C1-CGCZr$_2$ + B$_2$, ∼8× for C2-CGCZr$_2$ + B$_2$, and ∼11× for CGCZr$_1$ + B$_2$ (Table 1, entries 16−18), again suggesting that the "freer" cationic species generated in higher dielectric solvents are more accessible to the relatively bulky comonomers. In addition, C2-CGCZr$_2$ supported on highly Brønsted acidic sulfated alumina (Chart 2) is successfully activated by this support; however, the ligand and the steric

Chart 2. C2-CGCZr$_2$ Chemisorbed on Sulfated Alumina

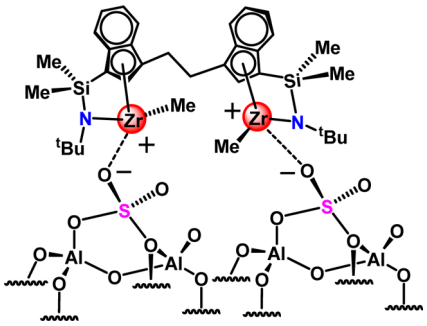

encumbrance of the support significantly depress catalytic activity.[21] These supported catalysts produce ultrahigh M_w polyethylene, in remarkable contrast to the homogeneous system which produces low M_w polyethylene. Ethylene/1-hexene copolymerizations show low levels of comonomer incorporation, again attributable to the steric bulk surrounding the bimetallic surface complex versus the more open environment in solution.

Copolymerizations of ethylene + 1-octene[27] or + a wide range of severely encumbered isoalkenes[28] mediated by bimetallic C2-CGCTi$_2$ are found to result in far greater densities of comonomer enchainment than does mononuclear CGCTi$_1$. Thus, C2-CGCTi$_2$ + B$_2$ enchains ∼11× more 1-octene in ethylene + 1-octene copolymerizations than does CGCTi$_1$ + B$_1$ under identical reaction conditions (Table 2, entries 1−4). Note that the activity of these CGCTi catalysts activated by trityl borates is ∼100× greater, and the product M_w is ∼100× greater than that achieved with the Zr analogues. However, ethylene + isobutene copolymerizations in the presence of trityl borate activators initiate cationic isobutene homopolymerization, yielding physical mixtures of polyethylene and polyisobutene homopolymers in the presence of C2-CGCTi$_2$ or CGCTi$_1$ (Table 2, entries 5−8). The same precatalysts have low activity with MAO, but C2-CGCTi$_2$ does incorporate ∼2× more isobutene into the copolymer than does CGCTi$_1$ (Table 2, entries 9, 10). In contrast, copolymerizations with borane cocatalysts afford ethylene + isobutene copolymers with good activities, and C2-CGCTi$_2$ + BN$_2$ incorporates ∼1.6× more isobutene than does CGCTi$_1$ (Table 2, entries 6, 8). For ethylene + methylene cyclopentane (MCP) or ethylene + methylene cyclohexane (MCH) copolymerizations, CGCTi catalysts cleanly incorporate the hindered comonomers in a ring-unopened regiochemistry, yielding copolymers via single-site enchainment processes (Scheme 4). Importantly, during polymerization the two metal centers can approach each other with an estimated minimum distance of ca. 3 Å, allowing the MCP and MCH comonomers to interact with both metal centers by means of M···olefin π-coordination and C−H···M agostic interactions, as suggested in Scheme 4. Again, the bimetallic catalysts/cocatalysts significantly enhance the encumbered comonomer enchainment selectivity versus the mononuclear analogues under identical reaction conditions.

The present bimetallic catalysts also produce otherwise inaccessible polymer microstructures as exemplified by the regiochemistry of styrene polymerizations mediated by C2-CGCTi$_2$.[29] The low styrene homopolymerization activity of CGCTi$_1$ is thought to reflect deactivation via intramolecular arene coordination in the 2,1-insertion product (Scheme 5, insert). However, for C2-CGCTi$_2$, the arene ring of the last inserted styrene may preferentially coordinate to the adjacent Ti center, reducing coordinative saturation at the polymerization site and accelerating homopolymerization by ∼39×. Among the possible styrene enchainment regiochemistries, while

dx.doi.org/10.1021/ar5001633 | Acc. Chem. Res. 2014, 47, 2545−2557

Table 2. Ethylene Copolymerization Characteristics for $CGCTi_1$ versus C2-$CGCTi_2$[a]

entry	catalyst	cocatalyst	comonomer	comonomer conc (M)	activity[b]	comonomer incorp (%)[c]	M_w (kg/mol)[d]	M_w/M_n[d]
1	$CGCTi_1$	B_1	1-octene	0.64	10 000	0.6	155	2.3
2	$CGCTi_1$	B_2	1-octene	0.64	3900	1.1	147	1.99
3	C2-$CGCTi_2$	B_1	1-octene	0.64	4300	1.0	157	2.75
4	C2-$CGCTi_2$	B_2	1-octene	0.64	3000	7.0	161	2.73
5	$CGCTi_1$	BN	isobutene	1.2	960	3.1	577	2.13
6	$CGCTi_1$	BN_2	isobutene	1.2	440	9.5	305	2.16
7	C2-$CGCTi_2$	BN	isobutene	1.2	490	7.3	490	2.41
8	C2-$CGCTi_2$	BN_2	isobutene	1.2	280	15.2	168	3.7
9	$CGCTi_1$	MAO	isobutene	1.2	39	2.9	487	2.5
10	C2-$CGCTi_2$	MAO	isobutene	1.2	44	6.2	355	2.9
11	$CGCTi_1$	BN	MCP	1.6	800	8.3	503	2.4
12	$CGCTi_1$	BN_2	MCP	1.6	660	14.8	285	1.9
13	C2-$CGCTi_2$	BN	MCP	1.6	730	13.3	342	2.1
14	C2-$CGCTi_2$	BN_2	MCP	1.6	590	20.4	186	2.3
15	$CGCTi_1$	BN	MCH	1.4	1300	3.3	475	1.8
16	C2-$CGCTi_2$	BN_2	MCH	1.4	350	8.3	369	2.8
17	$CGCTi_1$	BN	2-methyl-2-butene	2.7	730	1.1	769	2.0
18	C2-$CGCTi_2$	BN_2	2-methyl-2-butene	2.7	560	2.5	503	1.9
19	$CGCTi_1$	B_1	styrene	1.45	2200	28.0	76	1.4
20	C2-$CGCTi_2$	B_1	styrene	1.45	5800	32.3	367	2.2
21	$CGCTi_1$	B_1	4-methylstyrene	1.26	24 700	23.2	214	1.2
22	C2-$CGCTi_2$	B_1	4-methylstyrene	1.26	28 800	29.9	123	3.3
23	$CGCTi_1$	B_1	4-fluorostyrene	1.40	13 100	20.5	321	2.1
24	C2-$CGCTi_2$	B_1	4-fluorostyrene	1.40	5900	29.8	226	1.7
25	$CGCTi_1$	B_1	4-chlorostyrene	1.39	3100	14.8	77	1.9
26	C2-$CGCTi_2$	B_1	4-chlorostyrene	1.39	3100	20.9	855	1.7
27	$CGCTi_1$	B_1	4-bromostyrene	1.27	4400	12.9	150	4.0
28	C2-$CGCTi_2$	B_1	4-bromostyrene	1.27	5200	16.9	665	1.7

[a]Polymerizations carried out in 100 mL of toluene with 5 μmol of metal catalyst, at a constant 1.0 atm ethylene. [b]kg PE mol $[Ti]^{-1}$ atm^{-1} h^{-1}. [c]From ^{13}C NMR spectra. [d]GPC versus polystyrene standards; all distributions are monomodal.

Scheme 4. Proposed Scenario for Enhanced Methylenecycloalkanes Enchainment by Bimetallic Group 4 Catalysts

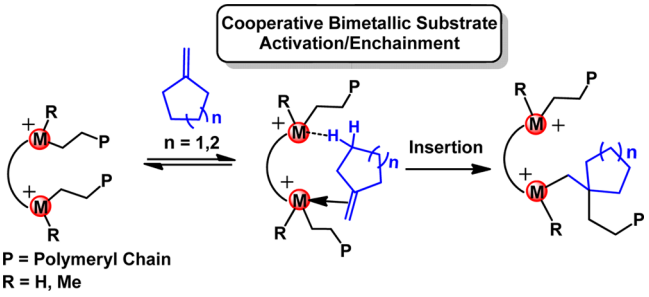

$CGCTi_1$ only participates in 2,1-insertion, C2-$CGCTi_2$ yields both 2,1-insertion and 1,2-insertion products (Scheme 5). In copolymerizations of ethylene + styrene or functionalized styrene comonomers,[30] the bimetallic catalysts are far more effective in comonomer enchainment. Under identical polymerization conditions, C2-$CGCTi_2$ + B_1 incorporates 15.4% more styrene than does mononuclear $CGCTi_1$ + B_1 (Table 2, entries 19, 20). With the 4-methylstyrene, 4-fluorostyrene, 4-chlorostyrene, and 4-bromostyrene comonomers, it is found that stronger metal−arene interaction, as NMR-indexed by the benzylic *ipso* ^{13}C chemical shift, correlates with more efficient styrenic comonomer enchainment by C2-$CGCTi_2$ versus $CGCTi_1$.

The scope and mechanism of alkenylsilanes as bifunctional comonomers for ethylene copolymerizations was also investigated with activated C2-$CGCTi_2$ and $CGCTi_1$.[31,32] As a comonomer, alkenylsilanes undergo both C═C insertion into growing polymer chains and serve as σ-bond metathesis chain transfer agents (Scheme 6; e.g., M−P + ≡Si−H → M−H + ≡Si−P). The chain transfers result in chain termination and facilitate reinsertion of the growing polymer chain, which effectively modulates M_n while simultaneously introducing functionality at the macromolecule chain ends. It is found that the above two Ti catalysts mediate alkenylsilane chain transfers in dramatically different ways depending on the alkenyl chain length, and that both catalysts produce silane-capped polyolefins. In particular, for shorter alkenylsilanes (C3 and C4) in the presence of the C2-$CGCTi_2$ catalyst, the standard chain-transfer plot of M_n versus $[silane]^{-1}$ reveals that M_n falls sublinearly with increasing alkenylsilane concentration. However, longer alkenylsilanes exhibit a superlinear relationship between product M_n and $[silane]^{-1}$. It is proposed that the longer silyl branches maximize the interchain chain transfer probability which in turn enhances the selectivity for alkenylsilane-branch chain transfer. In ethylene/alkenylsilane copolymerizations, bimetallic C2-$CGCTi_2$ generally produces higher M_n polymer but at somewhat lower activity versus mononuclear $CGCTi_1$ (Table 3). The increased M_n likely reflects cooperative enchainment/chain-transfer processes involving the proximate active metal centers, resulting in more probable macromonomer reinsertion and/or alkenylsilane-branch chain transfer to a growing chain (Scheme 6). The bimetallic C2-$CGCTi_2$ catalyst-mediated copolymerization/chain-transfer processes display an intricate, nonlinear dependence of M_n on inverse silane concentration, in contrast to all the previously studies alkyl- and arylsilane

dx.doi.org/10.1021/ar5001633 | Acc. Chem. Res. 2014, 47, 2545−2557

Scheme 5. Possible Insertion Pathways for Styrene Polymerization with Bimetallic C2-CGCTi$_2$; Inset Shows Inactive Monometallic Species

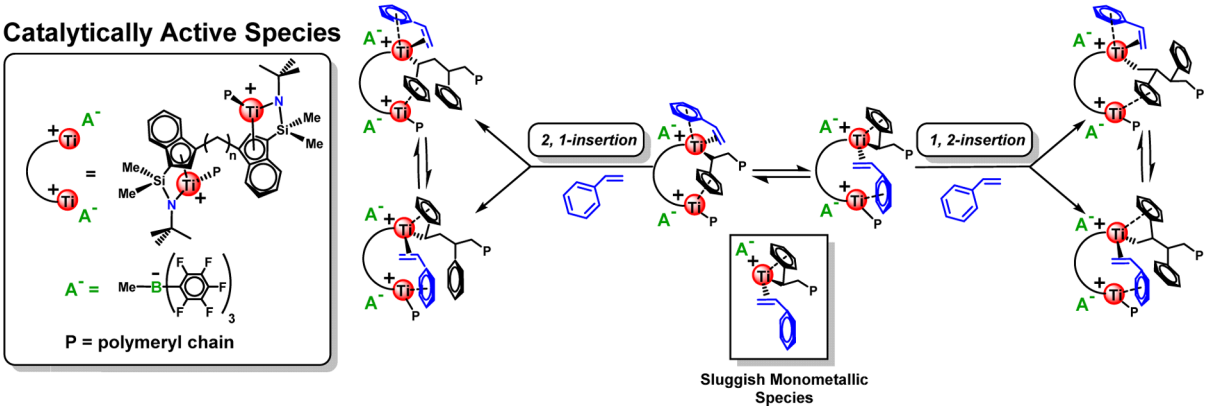

Scheme 6. Proposed Catalytic Cycle for C2-CGCTi$_2$-Mediated Ethylene/Alkenylsilane Copolymerizations

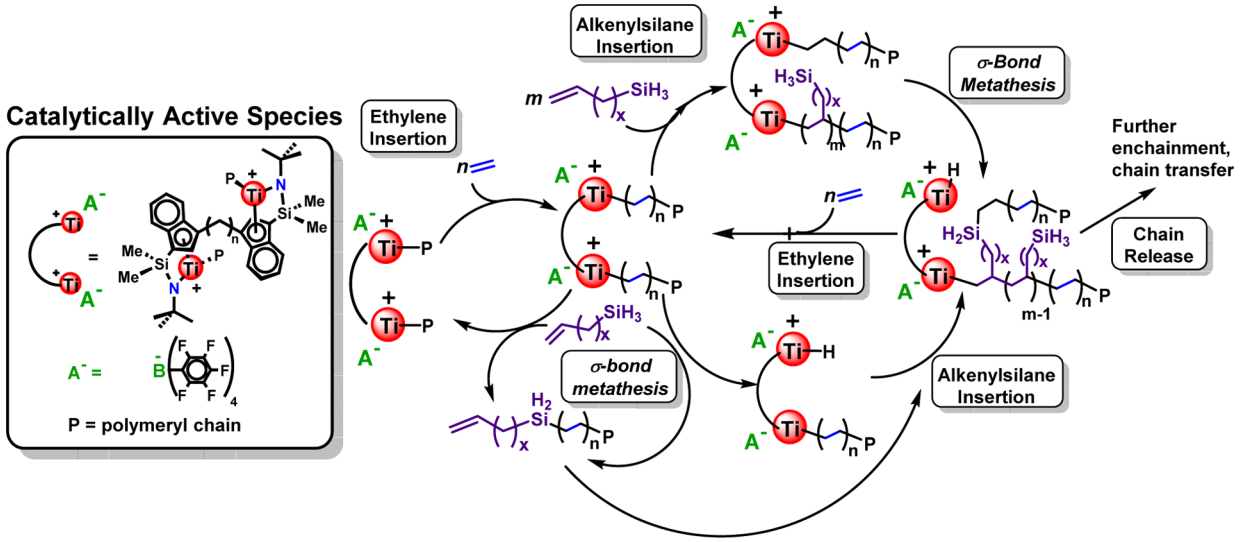

Table 3. Ethylene + Alkenylsilane Copolymerization Data Mediated by CGCTi$_1$ and C2-CGCTi$_2$[a]

entry	catalyst	comonomer	comonomer conc (mM)	activity[b]	comonomer incorp (%)[c]	M_n (kg/mol)[d]	M_w/M_n[d]
1	CGCTi$_1$	5-hexenylsilane	25.5	2900	1.0	43.9	2.6
2	C2-CGCTi$_2$	5-hexenylsilane	25.5	13.1	2.0	12.5	2.3
3	CGCTi$_1$	allylsilane	121	17 000	54	3.61	3.6
4	C2-CGCTi$_2$	allylsilane	121	5000	12	14.4	2.4
5	CGCTi$_1$	3-butenylsilane	110	19 000	20	2.3	4.2
6	C2-CGCTi$_2$	3-butenylsilane	110	0.2	5	82	2.0
7	CGCTi$_1$	7-octenylsilane	101	2	4	8.4	2.5
8	C2-CGCTi$_2$	7-octenylsilane	101	1	2	6.0	2.4

[a]Polymerizations carried out in 50 mL of toluene with 10 μmol of metal catalyst, 10 μmol of cocatalyst B$_1$, at a constant 1.0 atm ethylene. [b]In units of kg PE mol [Ti]$^{-1}$ atm^{-1} h^{-1}. [c]From ^{13}C NMR data. [d]GPC versus polyethylene standards.

systems[29,30] where the chain-transfer process is well-behaved with a linear relationship of M_n to [silane]$^{-1}$.

3. BIMETALLIC PHENOXYIMINATO POLYMERIZATION CATALYSTS

To explore the scope of center−center cooperative effects in coordinative olefin polymerizations, a new rigid, nonmetallocene bimetallic ligand scaffold was designed which holds the metal centers in closer proximity (~5.9 Å) than the CGC systems, and in a fixed position (Scheme 7). The phenoxyiminato ligand system which was used to great effect by Fujita et al.[33,34] and Grubbs et al.[35] was adapted to a bimetallic version. Binuclear ligand precursors[36] were synthesized by condensing 2,7-diformyl-1,8-dihydroxynaphthalene with 2,6-diisopropylaniline in refluxing CH_2Cl_2. The reagent 2,7-di(2,6-diisopropylphenyl)imino-1,8-di(trimethylsiloxy)-naphthalene is then generated by $LiCH_2TMS$ deprotonation, followed by TMSCl silylation. Note that direct addition of $ZrCl_4$ to the lithiated bisphenoxyiminato ligands proceeds in poor yields, likely yielding unreactive monometallic M(μ-O)M structures. Therefore, bimetallic precursor FI^2-M$_2$

dx.doi.org/10.1021/ar5001633 | Acc. Chem. Res. 2014, 47, 2545−2557

Scheme 7. Bisphenoxyiminato Ligand and Group 4 Complex Synthesis; Inset Shows Monometallic Analogue

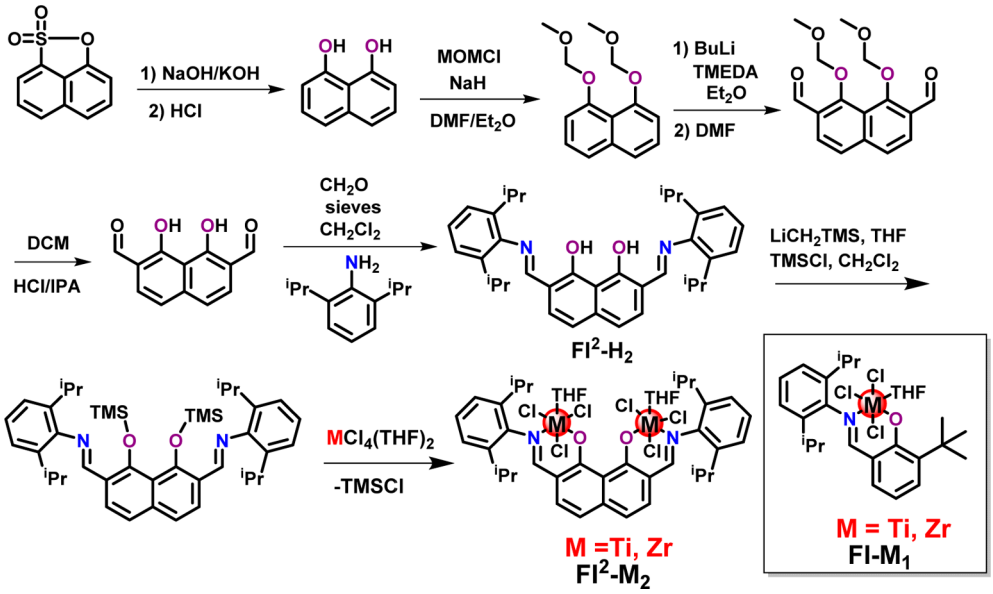

Table 4. Ethylene Homo- and Copolymerizations Mediated by FI^2-Zr_2, FI^2-Ti_2, FI-Zr_1, and FI-Ti_1[a]

entry	catalyst	comonomer	activity[b]	comonomer incorp (%)[c]	M_w (kg/mol)[g]	M_w/M_n[g]
1	FI^2-Zr_2		16		too insol.	
2	FI-Zr_1		2.1		too insol.	
3	FI^2-Ti_2		5.3		too insol.	
4	FI-Ti_1		2.5		675	23.7
5	FI^2-Zr_2[d]	1-hexene	12	11.0	98	3.31
6	FI-Zr_1[d]	1-hexene	1.0	7.4	21	9.61
7	FI^2-Ti_2[d]	1-hexene	4.5	9.4	76	3.91
8	FI-Ti_1[d]	1-hexene	2.7	4.3	188	33.6
9	FI^2-Zr_2[e]	MCP	6.9	PE		
10	FI-Zr_1[e]	MCP	3.3	PE		
11	FI^2-Ti_2[e]	MCP	15	0.7	121	4.01
12	FI-Ti_1[e]	MCP	3.4	0.4	58	20.2
13	FI^2-Zr_2[e]	MCH	6.2	PE		
14	FI-Zr_1[e]	MCH	2.6	PE		
15	FI^2-Ti_2[e]	MCH	9.7	11.6	104	3.48
16	FI-Ti_1[e]	MCH	8.1	3.4	20	13.1
17	FI^2-Zr_2[f]	1,5-HD	15	10.3	78	3.22
18	FI-Zr_1[f]	1,5-HD	1.0	7.9	34	10.3
19	FI^2-Ti_2[f]	1,5-HD	0.2			
20	FI-Ti_1[f]	1,5-HD	0.3			
21	FI^2-Zr_2[f]	1,4-PD	74	5.4	75	4.81
22	FI-Zr_1[f]	1,4-PD	29	2.1	73	3.28
23	FI^2-Ti_2[f]	1,4-PD	0.8			
24	FI-Ti_1[f]	1,4-PD	0.7			

[a]Polymerizations carried out on high vacuum line with MAO as cocatalyst (Al:Zr = 1000:1) in 50 mL of toluene with 10 μmol catalyst, at constant 1 atm ethylene pressure at 24 °C. Ethylene homopolymerizations for 60 min; ethylene copolymerizations for 45−75 min. [b]In units of kg polymer mol $[M]^{-1}$ atm^{-1} h^{-1}. [c]From ^{13}C NMR. [d]Polymerization at 40 °C. [e]Polymerization in neat comonomer. [f]Copolymerization with 0.3 M comonomer. [g]GPC versus polystyrene standard. PE = polyethylene.

is synthesized via TMSCl elimination using $MCl_4(THF)_2$ (M = Ti, Zr) in dichloromethane.

Ethylene homopolymerizations using the FI^2-Zr_2 precatalyst activated with MAO afford high-M_w linear (unbranched) polyethylenes with activities ∼8× that of mononuclear FI-Zr_1 (Table 4, entries 1 and 2). Interestingly, under the same conditions, FI^2-Ti_2[37] is less active than FI^2-Zr_2 (Table 4, entry 3), although the bimetallic catalyst is still ca. 2× more active than FI-Ti_1 (Table 4, entry 4). Furthermore, ethylene + 1-hexene copolymerizations with FI^2-Zr_2 result in efficient 1-hexene coenchainment with 1.5× the comonomer incorporation of mononuclear FI-Zr_1 (Table 4, entries 5 and 6). Again, the enhanced α-olefin coenchainment selectivity reflects the influence of the proximate metal center. A similar trend is observed in ethylene copolymerizations catalyzed by FI^2-Ti_2, where the bimetallic catalyst coenchains 2.2× more 1-hexene than does FI-Ti_1 (Table 4, entries 7 and 8).

The copolymerization characteristics of FI^2-M_2 catalysts were further explored with two additional comonomer classes. Highly

dx.doi.org/10.1021/ar5001633 | Acc. Chem. Res. 2014, 47, 2545−2557

Chart 3. Comonomers Introducing Saturated Hydrocarbon Ring Structures in the Product Polymer

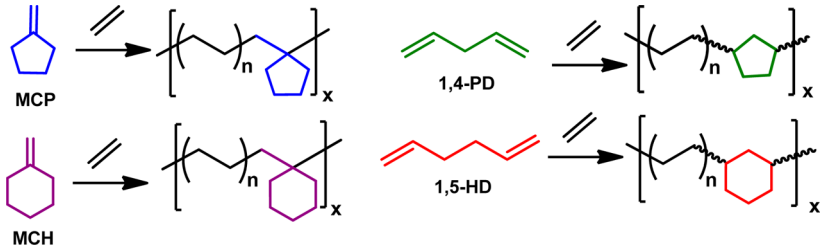

Scheme 8. Synthesis of Heterobimetallic Catalyst CGCTiZr

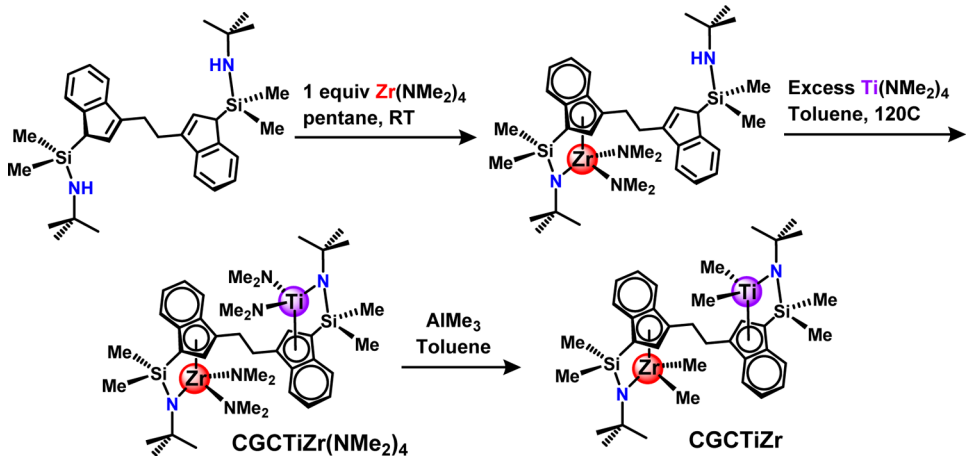

encumbered methylene cycloalkanes having minimal ring strain such as methylene cyclopentane (MCP) and methylene cyclohexane (MCH) are found to be suitable comonomers for ethylene copolymerization, leaving the hydrocarbon ring structures intact in the polymeric product (Chart 3). Such macromolecules are expected to have usefully modified viscoelastic properties because the bulky rings inhibit the tight coiling effects normally displayed by polyethylenes. Ethylene copolymerization experiments with MCP + FI^2-Ti_2 and FI-Ti_1 result in a low selectivity for comonomer incorporation (<1%), indicating a substantial barrier to MCP enchainment (Table 4, entries 11 and 12). Under identical reaction conditions, MCH is incorporated to a far greater extent with both FI^2-Ti_2 (11.6%, Table 4, entry 15) and FI-Ti_1 (3.4%, Table 4, entry 16). The proposed mechanistic scenario for enhanced methylene cycloalkene enchainment includes olefin coordination to one metal center and an agostic interaction with the second metal (Scheme 4). Interestingly, however, Zr catalysts FI^2-Zr_2 and FI-Zr_1 (Table 4, entries 9, 10, 13, and 14) do not enchain significant quantities of MCP or MCH, revealing a marked metal center dependence of the enchainment selectivity, possibly reflecting tighter ion-pairing with the associated MAO counteranions thereby raising the barrier to activation/insertion of these encumbered olefins.

A second comonomer class which can potentially introduce saturated hydrocarbon ring structures into polyethylene chains are α,ω-dienes such as 1,5-hexadiene (1,5-HD) and 1,4-pentadiene (1,4-PD) (Chart 3). These copolymerizations are distinct from the methylene cycloalkane systems in that FI^2-Zr_2 and FI-Zr_1 are far more effective than FI^2-Ti_2 and FI-Ti_1, which produce negligible copolymer under identical reaction conditions; it is possible that the larger Zr(IV) ionic radius versus Ti(IV) provides the spatial unsaturation required for diene coenchainment. Compared to FI-Zr_1, FI^2-Zr_2 enchains 1.3× more 1,5-HD at an activity which is 15.3× greater (Table 4, entries 17 and 18). Moreover, the copolymer ^{13}C NMR spectra indicate that both Zr catalysts convert all 1,5-HD units into a mixture of enchained *cis*- and *trans*-1,3-cyclohexyl fragments. With ethylene and 1,4-PD copolymerizations, FI^2-Zr_2 is 2.5× more active and incorporates 2.6× more comonomer than does FI-Zr_1 (Table 4, entries 21 and 22). ^{13}C NMR spectra once again indicate that all 1,4-PD units are a mixture of *cis*- and *trans*-1,3-cyclopentyl groups.

4. HETEROBIMETALLIC POLYMERIZATION CATALYSTS

An intriguing question in bimetallic catalysis is how cooperative effects might be altered when two *mechanistically very dissimilar* catalytic centers are held in close proximity. Although challenging to synthesize, heterobimetallic polymerization catalysts can create unique macromolecular polymer products from a single feedstock. The first covalently linked heterobimetallic polymerization catalyst CGCTiZr,[38] based on the constrained geometry ligand is prepared (Scheme 8) by sequential metalation, first with $Zr(NMe_2)_4$ and then with $Ti(NMe_2)_4$. After purification, the product $CGCTiZr(NMe_2)_4$ is alkylated with $AlMe_3$ to yield precatalyst CGCTiZr, in modest yield. The crystal structure of

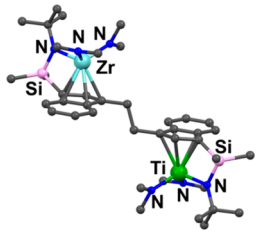

Figure 3. Molecular structure of $CGCTiZr(NMe_2)_4$ by single-crystal diffraction. Adapted with permission from ref 37. Copyright 2004 American Chemical Society.

dx.doi.org/10.1021/ar5001633 | *Acc. Chem. Res.* 2014, 47, 2545−2557

Table 5. Data for Ethylene Polymerizations Mediated by CGCTiZr[a]

entry	catalyst	conditions[b]	activity PE[c]	branches (/1000C)[d]	M_w (kg/mol)[e]	PDI[e]
1	CGCTiZr	24, 5	520	0	779	2.09
2	CGCTiZr	44, 3	1100	1.0	929	1.39
3	CGCTiZr	64, 1	2800	2.1	782	1.64
4	CGCZr	24, 15	140	0.7	0.730	1.10
5	CGCZr	64, 4	1400	0.8	0.690	1.20
6	CGCTi	24, 1	10 000	0	171	2.31
7	CGCTi	64, 1	15 000	0	121	1.64
8	CGCTi + CGCZr	64, 1	2800	0	238; 0.650	2.54; 1.30

[a]Polymerizations were carried out in 100 mL of toluene under 1.0 atm of ethylene; the catalyst loading was 10 μmol, with trityl tetrakis(pentafluorophenyl)borate as cocatalyst. [b]Conditions given: temperature of polymerization in °C, reaction time in min. [c]In units of g of polymer/[(mol of metal) atm h]. [d]From GPC with universal calibration using polystyrene standards. [e]Long chain branches (≥C6) calculated from ^{13}C NMR.

Table 6. Data for Ethylene Polymerizations Mediated by CGCTi, CGCTiCl$_2$-SNS, SNSCr, and TiCr[a]

entry	catalyst	PE (g)	activity (PE)[b]	oligomers (g)[c]	activity (oligomers)[d]	ρ_{br}[e]	M_n (kg·mol^{-1})[f]	PDI[f]	T_m (°C)
1	CGC^{Et}Ti	6.500	975.0			0	16.8	2.5	128.4
2	SNSCr	0.045	6.7	0.490	73.5	0	65.3	2.2	133.6
3	CGCTiCl$_2$-C$_0$-SNS	0.165	24.7			0	78.5	2.1	137.6
4	CGCTiCl$_2$-C$_2$-SNS	0.054	8.1			0	24.0	3.2	136.8
5	CGCTiCl$_2$-C$_6$-SNS	0.077	11.5			0	40.0	1.6	132.0
6	CGC^{Et}Ti + SNSCr	3.200	480.0	0.204	30.6	6.4	11.4	2.3	125.9
7	Ti-C$_0$-Cr^{SNS}	0.820	123.0	0.491	73.7	25.8	237	2.5	123.9
8	Ti-C$_2$-Cr^{SNS}	0.184	27.6	0.075	11.3	18.2	184	2.5	123.5
9	Ti-C$_6$-Cr^{SNS}	0.134	20.1	0.066	9.9	6.8	127	2.5	126.0

[a]Polymerizations carried out in 50 mL of toluene with 10 μmol of each component catalyst, at constant 8.0 atm ethylene pressure at 80 °C for 5 min, using 500 equiv of MAO as cocatalyst. [b]In units of (kg of PE) (mol of catalyst)$^{-1}$ atm^{-1} h^{-1}. [c]Determined by GC-TOF with mesitylene as an internal standard. Selectivity for 1-hexene from 53% (entry 3) to 98% (entry 5) [d]Determined by ^{13}C NMR. [e]Differential scanning calorimetry [f]Triple detection GPC.

Scheme 9. Proposed Cooperative Enchainment at Heterobinuclear Catalyst CGCTiZr

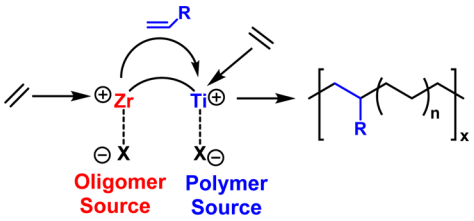

CGCTiZr reveals that the Ti and Zr atoms are positionally disordered (50%, Figure 3). The derived metal−ligand metrical parameters are essentially the average of those determined for similar homobinuclear Ti and Zr CGC complexes, while the internal ligand distances and angles are unexceptional. Nevertheless, the molecular constitution is verified by a combination of high-resolution MS, 2-D NMR spectroscopy, and elemental analysis.

Ethylene polymerization experiments show that CGCTiZr create high-M_w polyethylenes of 779 kg/mol with a high activity of 520 kg PE mol [M]$^{-1}$ atm^{-1} h^{-1} at room temperature (Table 5). At elevated temperatures, some long chain branching is noted in the product polymer. The differences in the polymer microstructure produced by catalyst CGCTiZr versus C2-CGCZr$_2$, C2-CGCTi$_2$, or the monometallic catalysts evidence marked cooperative effects. Specifically, the long chain branching indicates that the Ti metal is able to efficiently capture/enchain the sizable oligomers produced at the Zr center into the propagating Ti-polymer backbone (Scheme 9). Note that the activity of the Ti catalytic center is estimated to be ∼50× greater than that of the Zr center, consistent with the low branch densities observed in the product polyethylenes.

To explore accentuated metal dissimilarity effects on polymerization cooperativity, a series of Cr−Ti heterobimetallic catalysts were synthesized which contain an active ethylene trimerization center, SNSCr, covalently linked to a CGCTi$_1$ unit, which produces high M_w polyethylenes with high activity and good comonomer selectivity (Scheme 10).[12,39] The Ti-C$_n$-Cr (n = 0, 2, 6) catalysts were characterized by standard analytical techniques and by the broad ^{1}H NMR features indicative of the paramagnetic Cr(III) center. In ethylene homopolymerizations, both the product M_w's and branch densities roughly scale inversely with metal···metal distance in the order, Ti-C$_0$-Cr^{SNS} > Ti-C$_2$-Cr^{SNS} > Ti-C$_6$-Cr^{SNS} > CGCTi + SNSCr, under identical polymerization conditions with an MAO cocatalyst in toluene. With ethylene as the only feed and MAO as the cocatalyst/activator, SNS-based complexes Ti-C$_0$-Cr^{SNS}, Ti-C$_2$-Cr^{SNS}, and Ti-C$_6$-Cr^{SNS} afford linear low-density polyethylenes (LLDPEs) with exclusive n-butyl branches (6.8−25.8 branches/1000C; Table 6). In addition, the branch density is essentially independent of reaction time and conversion despite increasing available concentrations of the free oligomer produced by the SNSCr unit. Note that the CGCTi-SNSCr-derived branch density is significantly higher than the 6.4 n-butyl branches/1000C produced by a tandem mixture of mononuclear CGCTi + SNSCr catalysts under identical reaction conditions, despite far higher free oligomer concentrations in the latter. In addition, under identical ethylene polymerization conditions, Ti-C$_0$-Cr^{SNS} produces polyethylenes with higher activity (4.5× and 6.1×, respectively), M_w (1.3× and 1.8×, respectively), and branch density (1.4× and 3.8×, respectively), than do Ti-C$_2$-Cr^{SNS} and Ti-C$_6$-Cr^{SNS}. Under the same experimental conditions,

dx.doi.org/10.1021/ar5001633 | Acc. Chem. Res. 2014, 47, 2545−2557

Scheme 10. Synthetic Scheme for the Heterobimetallic Polymerization Catalyst Ti-C_n-Cr; Inset Shows Structures of Monometallic Controls

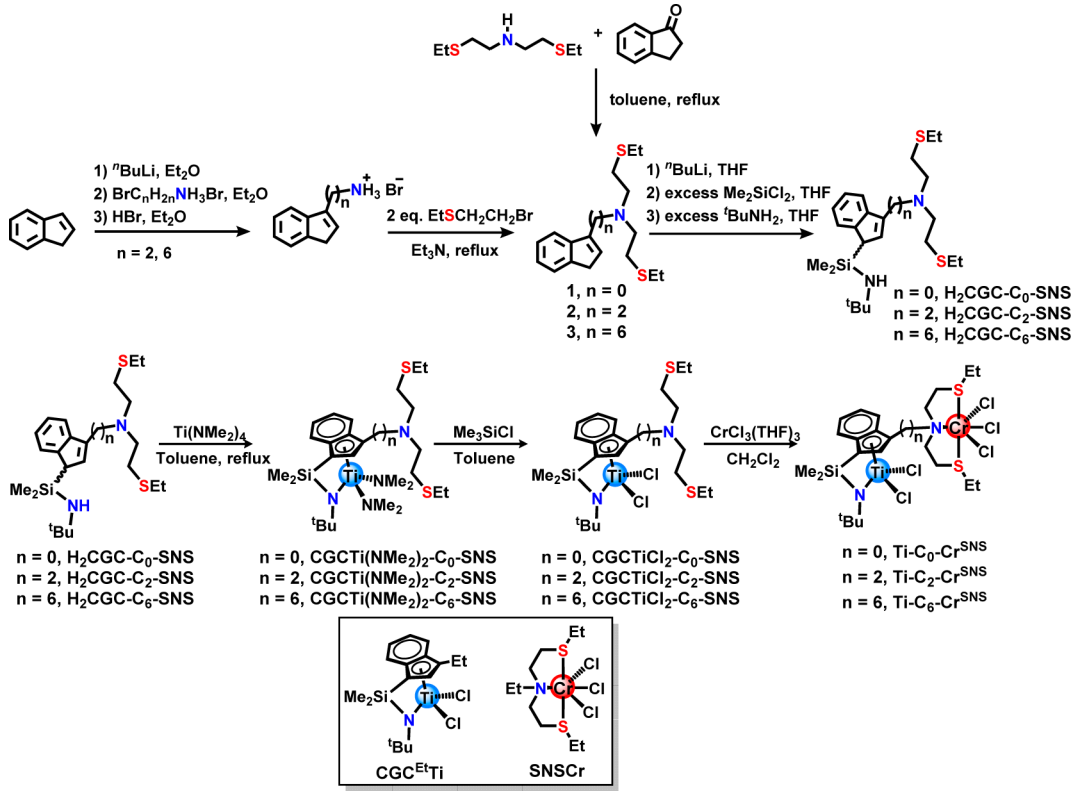

Scheme 11. Catalytic Cycle for Ethylene Polymerization Propagation and Chain Transfer Processes by CGCTi-SNSCr with DFT Computed Structure of 1-Hexene Binding

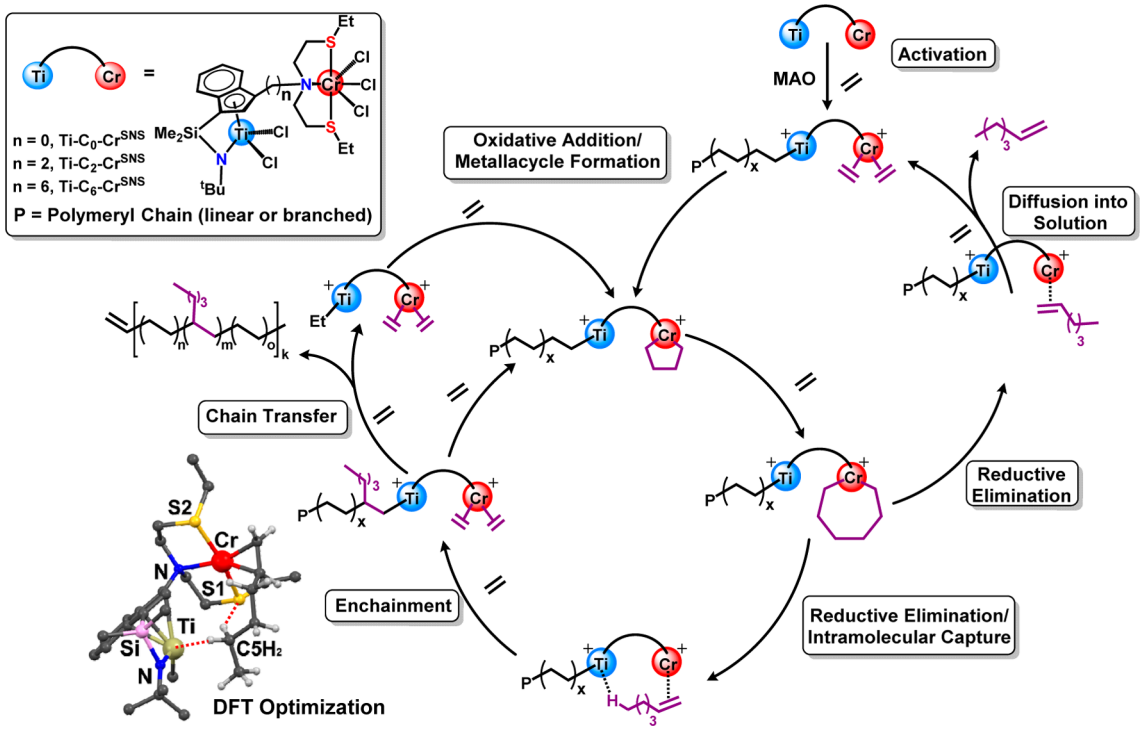

$Ti\text{-}C_0\text{-}Cr^{SNS}$ yields polyethylene with lower activity then the $CGC^{Et}Ti$ + SNSCr tandem catalyst, but with 22.6× higher M_w and 4.0× greater branching density. To further scrutinize the details of the 1-hexene transfer mechanism in Ti-C_n-Cr polymerizations, 0.10 M 1-pentene was added to the reaction mixtures and allowed to compete for enchainment with the 1-hexene produced at the Cr center. It is found that the CGCTi + SNSCr tandem system yields polymer with 68.0 branches/1000C atoms, 91% of which are

dx.doi.org/10.1021/ar5001633 | Acc. Chem. Res. 2014, 47, 2545−2557

n-propyl. Under identical conditions Ti-C_0-Cr produces polymer with 25.3 branches/1000C atoms, of which only 5.5% are *n*-propyl and the 1-hexene enchainment density is virtually unaffected versus experiments without 1-pentene.[12,39] These results argue that Ti-C_n-Cr spatially confines the catalytic centers in such a way that the efficiency of intramolecular comonomer transfer to, and enchainment at, CGCTi is highly selective for the C_6 comonomer. A catalytic cycle is proposed (Scheme 11) where C_6 fragments are produced at the SNSCr center by established sequences of reductive ethylene coupling and metallacyclopentane expansion to a metallacycloheptane, followed by reductive elimination to yield 1-hexene which is subsequently captured by the CGCTi center, probably in a concerted fashion. DFT calculations support this hypothesis and identify an energetic minimum in which 1-hexene is π-bound to the Cr center while engaging in a −CH···Ti agostic interaction and weak C−H···S interactions (Scheme 11).[12,39]

5. CONCLUSIONS AND PROSPECTS

This Account analyzes the effects on monomer enchainment/coenchainment processes at single-site olefin polymerization catalysts having a second catalytic center within close proximity. It is seen that proximity-based cooperative enchainment effects result in marked alterations in catalytic activity, product macromolecule mass and architecture, and comonomer enchainment selectivity. These effects are greatest in the case of close M···M contacts and are appreciably modulated by the supporting ligation, cocatalyst-derived counteranion, and solvent. With heterobimetallic ethylene polymerization catalysts, linear low density polyethylenes can be produced by a single ethylene feedstock via concerted transfer of low M_w α-olefins generated at one metal center to the other. Future efforts in bimetallic ethylene polymerization catalysis are focusing on heterobimetallic or heteroligated systems with increasing site dissimilarities and enhanced M···M communication.

AUTHOR INFORMATION

Corresponding Author

*E-mail: t-marks@northwestern.edu.

Notes

The authors declare no competing financial interest.

Biographies

Jennifer P. McInnis is from Acton, MA. She received a B.A. in Chemistry from Cornell University in 2008. She graduated with a Ph.D. in organometallic chemistry and olefin polymerization catalysis from Northwestern University in 2014 working under the supervision of Tobin J. Marks.

Massimiliano Delferro was born in 1981 in Parma, Italy. He received a B.S. degree in inorganic chemistry with honors and completed a Ph.D. in Chemical Sciences from the University of Parma under the supervision of Prof. D. A. Cauzzi. In 2009, he joined Northwestern University where he is currently a Research Associate Professor. Dr. Delferro's research interests include polyolefin synthesis and structure−activity/reactivity relationships in homo- and heterobinuclear single-site homogeneous polymerization catalysts, f-element chemistry and catalysis, and support organometallic chemistry on superacidic surfaces.

Tobin J. Marks was born in Washington, D.C.. He is currently Ipatieff Professor of Chemistry and Professor of Materials Science and Engineering at Northwestern University. He received a B.S. degree from the University of Maryland and Ph.D. from MIT in Chemistry. He is a member of the U.S. National Academy of Sciences, a Fellow of the American Academy of Arts and Sciences, a Member of the German National Academy of Sciences, and a Fellow of the Royal Society of Chemistry. Among other recognitions, he has received the U.S. National Medal of Science, the Spanish Principe de Asturias Prize, the Von Hippel Award of the Materials Research Society, and the Dreyfus Prize in the Chemical Sciences.

ACKNOWLEDGMENTS

The authors are grateful to NSF (Grant CHE-1213235; fundamental homogeneous catalysis) and DOE (Grant 86ER13511; the interface of heterogeneous and homogeneous catalysis) for generous support of this research.

REFERENCES

(1) Silanes, I.; Ugalde, J. M. Comparative Study of Various Mechanisms for Metallocene-Catalyzed α-Olefin Polymerization. *Organometallics* **2005**, *24*, 3233−3246.
(2) Weiss, H.; Ehrig, M.; Ahlrichs, R. Ethylene insertion in the homogeneous Ziegler-Natta catalysis: an ab initio investigation on a correlated level. *J. Am. Chem. Soc.* **1994**, *116*, 4919−4928.
(3) Zhang, W.; Sun, W.-H.; Zhang, S.; Hou, J.; Wedeking, K.; Schultz, S.; Fröhlich, R.; Song, H. Synthesis, Characterization, and Ethylene Oligomerization and Polymerization of [2,6-Bis(2-benzimidazolyl)-pyridyl]chromium Chlorides. *Organometallics* **2006**, *25*, 1961−1969.
(4) Cossee, P. Ziegler-Natta catalysis I. Mechanism of polymerization of α-olefins with Ziegler-Natta catalysts. *J. Catal.* **1964**, *3*, 80−88.
(5) Haak, R. M.; Wezenberg, S. J.; Kleij, A. W. Cooperative multimetallic catalysis using metallosalens. *Chem. Commun.* **2010**, *46*, 2713−2723.
(6) Yamatsugu, K.; Yin, L.; Kamijo, S.; Kimura, Y.; Kanai, M.; Shibasaki, M. A Synthesis of Tamiflu by Using a Barium-Catalyzed Asymmetric Diels−Alder-Type Reaction. *Angew. Chem., Int. Ed.* **2009**, *48*, 1070−1076.
(7) Sone, T.; Yamaguchi, A.; Matsunaga, S.; Shibasaki, M. Catalytic Asymmetric Synthesis of 2,2-Disubstituted Terminal Epoxides via Dimethyloxosulfonium Methylide Addition to Ketones. *J. Am. Chem. Soc.* **2008**, *130*, 10078−10079.
(8) Paull, D. H.; Abraham, C. J.; Scerba, M. T.; Alden-Danforth, E.; Lectka, T. Bifunctional Asymmetric Catalysis: Cooperative Lewis Acid/Base Systems. *Acc. Chem. Res.* **2008**, *41*, 655−663.
(9) Delferro, M.; Marks, T. J. Multinuclear Olefin Polymerization Catalysts. *Chem. Rev.* **2011**, *111*, 2450−2485.
(10) Li, H.; Marks, T. J. Nuclearity and cooperativity effects in binuclear catalysts and cocatalysts for olefin polymerization. *Proc. Natl. Acad. Sci. U.S.A.* **2006**, *103*, 15295−15302.
(11) Weberski, M. P.; Chen, C. L.; Delferro, M.; Marks, T. J. Ligand Steric and Fluoroalkyl Substituent Effects on Enchainment Cooperativity and Stability in Bimetallic Nickel(II) Polymerization Catalysts. *Chem.—Eur. J.* **2012**, *18*, 10715−10732.
(12) Liu, S.; Motta, A.; Delferro, M.; Marks, T. J. Synthesis, Characterization, and Heterobimetallic Cooperation in a Titanium−Chromium Catalyst for Highly Branched Polyethylenes. *J. Am. Chem. Soc.* **2013**, *135*, 8830−8833.
(13) Braunschweig, H.; Breitling, F. M. Constrained geometry complexes—Synthesis and applications. *Coord. Chem. Rev.* **2006**, *250*, 2691−2720.
(14) Vidyaratne, I.; Scott, J.; Gambarotta, S.; Duchateau, R. Reactivity of Chromium Complexes of a Bis(imino)pyridine Ligand: Highly Active Ethylene Polymerization Catalysts Carrying the Metal in a Formally Low Oxidation State. *Organometallics* **2007**, *26*, 3201−3211.
(15) Matsuhashi, H.; Motoi, H.; Arata, K. Determination of acid strength of solid superacids by temperature programmed desorption using pyridine. *Catal. Lett.* **1994**, *26*, 325−328.
(16) Chen, E. Y.-X.; Marks, T. J. Cocatalysts for Metal-Catalyzed Olefin Polymerization: Activators, Activation Processes, and Structure−Activity Relationships. *Chem. Rev.* **2000**, *100*, 1391−1434.

(17) Gao, R.; Liang, T.; Wang, F.; Sun, W.-H. Chromium(III) complexes bearing 2-benzoxazolyl-6-arylimino-pyridines: Synthesis and their ethylene reactivity. *J. Organomet. Chem.* **2009**, *694*, 3701−3707.
(18) Lanza, G.; Fragala, I. L.; Marks, T. J. Ligand Substituent, Anion, and Solvation Effects on Ion Pair Structure, Thermodynamic Stability, and Structural Mobility in "Constrained Geometry" Olefin Polymerization Catalysts: an Ab Initio Quantum Chemical Investigation. *J. Am. Chem. Soc.* **2000**, *122*, 12764−12777.
(19) Li, H.; Stern, C. L.; Marks, T. J. Significant Proximity and Cocatalyst Effects in Binuclear Catalysis for Olefin Polymerization. *Macromolecules* **2005**, *38*, 9015−9027.
(20) Motta, A. Private communication of DFT calculations, 2014.
(21) Williams, L. A.; Marks, T. J. Chemisorption Pathways and Catalytic Olefin Polymerization Properties of Group 4 Mono- and Binuclear Constrained Geometry Complexes on Highly Acidic Sulfated Alumina. *Organometallics* **2009**, *28*, 2053−2061.
(22) Yang, X.; Stern, C. L.; Marks, T. J. Cationic Zirconocene Olefin Polymerization Catalysts Based on the Organo-Lewis Acid Tris-(pentafluorophenyl)borane. A Synthetic,Structural, Solution Dynamic, and Polymerization Catalytic Study. *J. Am. Chem. Soc.* **1994**, *116*, 10015−10031.
(23) Chien, J. C. W.; Tsai, W. M.; Rausch, M. D. Isospecific Polymerization of Propylene Catalyzed by Rac-Ethylenebis(Indenyl)-Methylzirconium Cation. *J. Am. Chem. Soc.* **1991**, *113*, 8570−8571.
(24) Li, L.; Metz, M. V.; Li, H.; Chen, M.-C.; Marks, T. J.; Liable-Sands, L.; Rheingold, A. L. Catalyst/Cocatalyst Nuclearity Effects in Single-Site Polymerization. Enhanced Polyethylene Branching and α-Olefin Comonomer Enchainment in Polymerizations Mediated by Binuclear Catalysts and Cocatalysts via a New Enchainment Pathway. *J. Am. Chem. Soc.* **2002**, *124*, 12725−12741.
(25) Li, H.; Li, L.; Marks, T. J. Polynuclear olefin polymerization catalysis: Proximity and cocatalyst effects lead to significantly increased polyethylene molecular weight and comonomer enchainment levels. *Angew. Chem., Int. Ed.* **2004**, *43*, 4937−4940.
(26) Motta, A.; Fragala, I. L.; Marks, T. J. Proximity and Cooperativity Effects in Binuclear d(0) Olefin Polymerization Catalysis. Theoretical Analysis of Structure and Reaction Mechanism. *J. Am. Chem. Soc.* **2009**, *131*, 3974−3984.
(27) Li, H.; Li, L.; Marks, T. J.; Liable-Sands, L.; Rheingold, A. L. Catalyst/Cocatalyst Nuclearity Effects in Single-Site Olefin Polymerization. Significantly Enhanced 1-Octene and Isobutene Comonomer Enchainment in Ethylene Polymerizations Mediated by Binuclear Catalysts and Cocatalysts. *J. Am. Chem. Soc.* **2003**, *125*, 10788−10789.
(28) Li, H. B.; Li, L. T.; Schwartz, D. J.; Metz, M. V.; Marks, T. J.; Liable-Sands, L.; Rheingold, A. L. Coordination copolymerization of severely encumbered isoalkenes with ethylene: Enhanced enchainment mediated by binuclear catalysts and cocatalysts. *J. Am. Chem. Soc.* **2005**, *127*, 14756−14768.
(29) Guo, N.; Li, L. T.; Marks, T. J. Bimetallic catalysis for styrene homopolymerization and ethylene-styrene copolymerization. Exceptional comonomer selectivity and insertion regiochemistry. *J. Am. Chem. Soc.* **2004**, *126*, 6542−6543.
(30) Guo, N.; Stern, C. L.; Marks, T. J. Bimetallic effects in homopolymerization of styrene and copolymerization of ethylene and styrenic comonomers: Scope, kinetics, and mechanism. *J. Am. Chem. Soc.* **2008**, *130*, 2246−2261.
(31) Amin, S. B.; Marks, T. J. Alkenylsilane structure effects on mononuclear and binuclear organotitanium-mediated ethylene polymerization: Scope and mechanism of simultaneous polyolefin branch and functional group introduction. *J. Am. Chem. Soc.* **2007**, *129*, 2938−2953.
(32) Amin, S. B.; Marks, T. J. Versatile Pathways for In Situ Polyolefin Functionalization with Heteroatoms: Catalytic Chain Transfer. *Angew. Chem., Int. Ed.* **2008**, *47*, 2006−2025.
(33) Makio, H.; Terao, H.; Iwashita, A.; Fujita, T. FI Catalysts for Olefin Polymerization—A Comprehensive Treatment. *Chem. Rev.* **2011**, *111*, 2363−2449.
(34) Makio, H.; Fujita, T. Development and Application of FI Catalysts for Olefin Polymerization: Unique Catalysis and Distinctive Polymer Formation. *Acc. Chem. Res.* **2009**, *42*, 1532−1544.
(35) Wang, C.; Friedrich, S.; Younkin, T. R.; Li, R. T.; Grubbs, R. H.; Bansleben, D. A.; Day, M. W. Neutral Nickel(II)-Based Catalysts for Ethylene Polymerization. *Organometallics* **1998**, *17*, 3149−3151.
(36) Salata, M. R.; Marks, T. J. Synthesis, Characterization, and Marked Polymerization Selectivity Characteristics of Binuclear Phenoxyiminato Organozirconium Catalysts. *J. Am. Chem. Soc.* **2008**, *130*, 12−13.
(37) Salata, M. R.; Marks, T. J. Catalyst Nuclearity Effects in Olefin Polymerization. Enhanced Activity and Comonomer Enchainment in Ethylene + Olefin Copolymerizations Mediated by Bimetallic Group 4 Phenoxyiminato Catalysts. *Macromolecules* **2009**, *42*, 1920−1933.
(38) Wang, J.; Li, H.; Guo, N.; Li, L.; Stern, C. L.; Marks, T. J. Covalently Linked Heterobimetallic Catalysts for Olefin Polymerization. *Organometallics* **2004**, *23*, 5112−5114.
(39) Liu, S.; Motta, A.; Mouat, A. R.; Delferro, M.; Marks, T. J. Very Large Cooperative Effects in Heterobimetallic Titanium-Chromium Catalysts for Ethylene Polymerization/Copolymerization. *J. Am. Chem. Soc.* **2014**, *136*, 10460−10469.